Pergamon

0301-9322(94)00075-1

Int. J. Multiphase Flow Vol. 21, No. 2, pp. 223–239, 1995
Copyright © 1995 Elsevier Science Ltd
Printed in Great Britain. All rights reserved
0301-9322/95 $9.50 + 0.00

PROPAGATION OF VOIDAGE WAVES IN A TWO-DIMENSIONAL LIQUID-FLUIDIZED BED

M. POLETTO, R. BAI and D. D. JOSEPH

Department of Aerospace Engineering and Mechanics, University of Minnesota, 107 Akerman Hall, 110 Union Street, Minneapolis, MN 55455, U.S.A.

(Received 3 April 1994; in revised form 12 October 1994)

Abstract—Digital video recordings were used to obtain voidage distribution in a narrow fluidized bed with a small gap slightly larger than three particle diameters. From these recordings we determined auto-correlations and power spectra in spatial and temporal and joint spatial–temporal power spectra. Increases in the fluidization velocity lead to increasing disorganized non-periodic flows. Our experimental results are discussed in the light of experimental results and theories found in literature.

Key Words: liquid fluidization, homogeneous fluidization, voidage instabilities, non-homogeneous fluidization, two-dimensional fluidized bed

INTRODUCTION

Beds fluidized with liquids tend to fluidize without bubbles (particulate fluidization). The bed expansion is very well represented by the Richardson & Zaki (1954) correlation which predicts a linear correlation between the logarithm of the fluid superficial velocity and the logarithm of the bed voidage. In beds fluidized with gases, spherical cavities, called bubbles, flow through the bed (aggregative fluidization) and the bed expansion is not well represented by the Richardson & Zaki (1954) equation.

Studies of liquid-fluidized beds by Anderson & Jackson (1969), El-Kaissy & Homsy (1976), Didwania & Homsy (1981) and by Ham *et al.* (1990) have shown that there may be local fluctuations in the bed voidage which propagate upwards in the bed and which make this kind of fluidization non-uniform. This kind of propagation is also seen in two-dimensional fluidized beds of macroscopic particles in which the gap size of the bed is equal to the particle diameter. Volpicelli *et al.* (1966) have observed the presence of horizontal cracks which propagate upwards in the bed. A fluid dynamic interpretation of this has been given by Joseph *et al.* (1987) who observed the formation of horizontal arrays of particles induced by pair interactions which they described as drafting, kissing and tumbling. Singh & Joseph (1991, 1995) used tools of statistical analysis to assess the effect of particle size on the voidage and area fraction distributions within the bed.

In this work, similar tools will be used to further characterize the phenomenology of onset and propagation of voidage disturbances in liquid fluidized beds. We used a narrow bed of plastic beads fluidized with water, whose gap was slightly larger than three particle diameters. A video recording technique similar to the one used by Singh & Joseph (1991, 1995) to study the temporal and spatial structure of voidage waves in a bed whose depth is a little larger than one particle diameter is extended here to beds which are three or four diameters deep. This technique yields new data which is compared with theoretical predictions.

EXPERIMENTAL

Apparatus

Figure 1 shows a sketch of the experimental apparatus. A fluidization column, C, 910 mm high, 70 mm wide and 18 mm deep was used. The front wall was transparent to allow an inside view of the bed, B. The back wall was opaque and black.

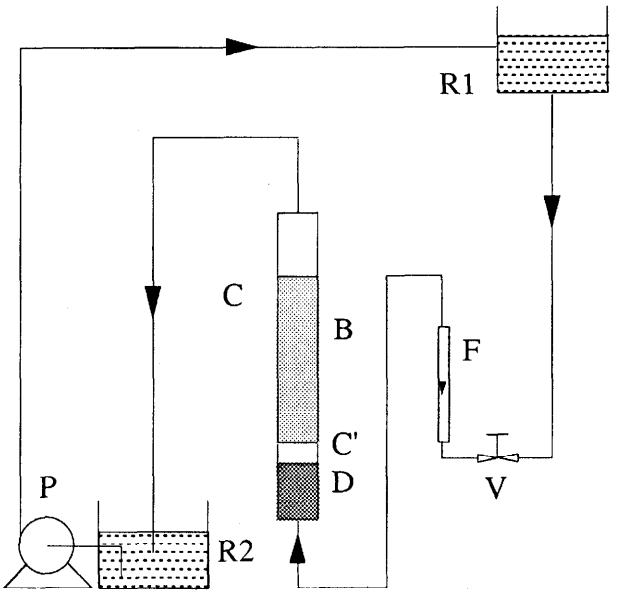

Figure 1. Experimental apparatus. B, Fluidized bed; C, column; C′, calming section; D, distributor; F, flow meter; P, pump; R1, upper water reservoir; R2, lower water reservoir; V, metering valve.

The bed was fluidized with water. To avoid the effects of pump pressure pulsation or tap water pressure variation, water was withdrawn from a reservoir, R1, suspended at ca. 16 m. The water flow rate was adjusted with a metering valve, V, and was measured with a calibrated rotameter, F. A satisfactory homogeneous distribution was achieved using a fixed bed, D, 120 mm high, of lead shots of 3 mm diameter kept confined downwards by a steel net. Another steel net, 20 mm higher, was used to suspend the fluidized bed. This method of suspension created a downstream calming section, C′. A pump, P, recirculated the water from the lower reservoir, R2, to the upper reservoir R1.

White plastic beads 6.35 mm diameter and 1210 kg m^{-3} were used. The bed depth was purposely chosen to be approximately three particle diameters so that, though the particles could move in three directions within the bed, local solid concentration could be visually observed. Photographs showing front and side views of the bed at three different levels of bed expansion are exhibited in figure 2. Non-linear interactions leading to the drafting, kissing and tumbling into across stream arrangements are in evidence in both front and side view [see Fortes *et al.* (1987) and Joseph *et al.* (1992)] of figure 2.

Procedure

Voidage (the volume fraction occupied by the fluid) was monitored as the black background in a bed of white beads. Video recordings of the bed fluidization were taken with a Kodak SP2000 digital video camera, which allowed acquisition and treatment of the images by a Macintosh personal computer. The black and white digital video camera SP2000 associated an integer between 0 and 255 at every pixel constituting the image according to the degree of brightness: 0 is black and 255 is bright white. The mean value of the brightness number was averaged over all the pixels in the video image of the bed. This mean value correlated with the mean solid concentration, $\phi = 1 - \epsilon$, which was evaluated from the bed height, H, using the equation $\phi = N_p V_p / A_c H$, where N_p is the number of particles in the bed, V_p is the particle volume and A_c is the fluidized bed cross-section.

Figure 3 shows the measured mean value of brightness in a fluidized bed with different mean solid concentrations under the same lighting condition. Particular care was taken to create a uniform distribution of light all over the bed. The correlation between values of mean concentration taken from the bed expansion and brightness number is good. The linear regression of experimental data, whose equation is given in the caption, gives a high value of the linear correlation coefficient,

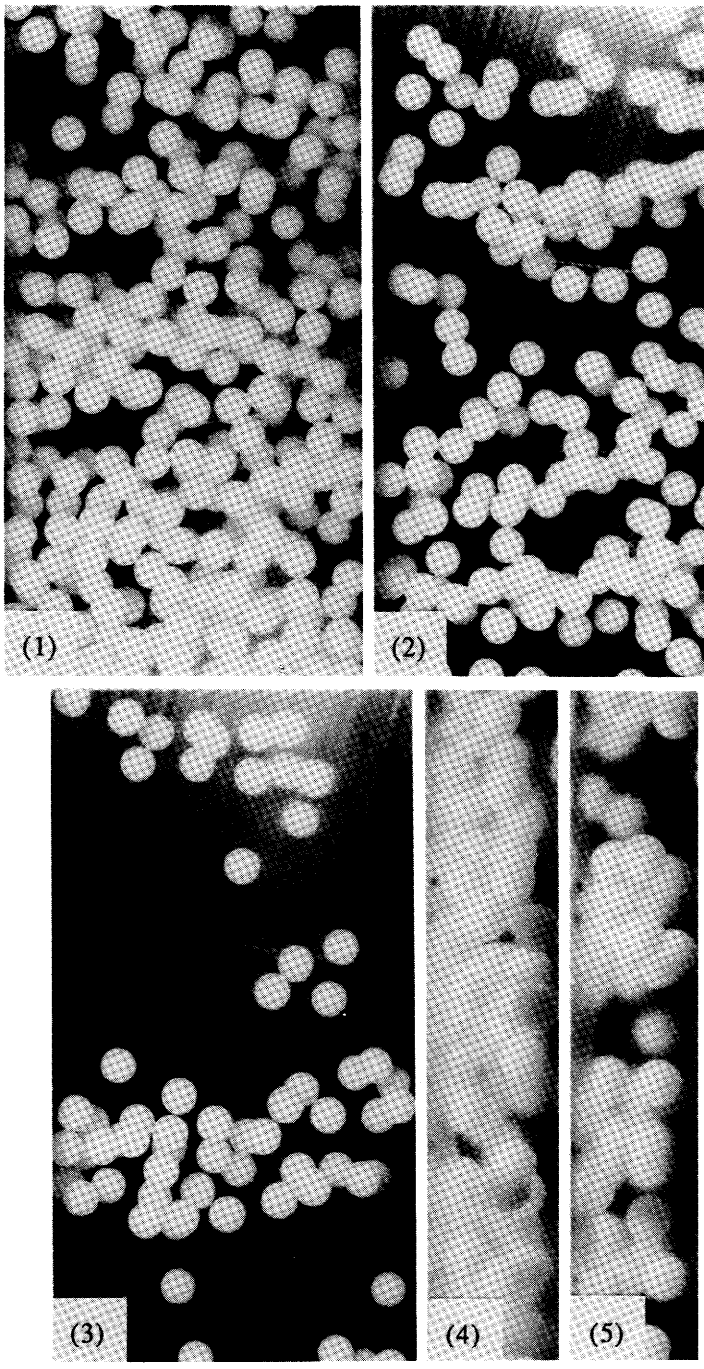

Figure 2. Front and side views of a fluidized bed. Front view: (1) $\epsilon = 0.73$, $U = 4.65\,\mathrm{cm\,s^{-1}}$; (2) $\epsilon = 0.83$, $U = 6.92\,\mathrm{cm\,s^{-1}}$; (3) high voidage and fluid velocity. Side view; (4) $\epsilon = 0.85$ $U = 7.10\,\mathrm{cm\,s^{-1}}$; (5) high voidage and fluid velocity. Cases (3) and (5) refer to fluid velocities much higher than those analyzed in the rest of the paper and therefore were not quantitatively characterized.

$r = 0.998$. Therefore a linear correlation is satisfactory to describe the correlation between voidage and brightness in the range of values under consideration and justifies the direct use of fluctuations of brightness values in the analysis of fluctuations of voidage. Voidage profiles were determined by averaging the brightness of all the pixels on a horizontal line at a certain height over the distributor. In this way we get a discrete representation of the profile on the number of pixel lines contained in the image of the bed. With the SP2000 video recording system the maximum value of this number was 238.

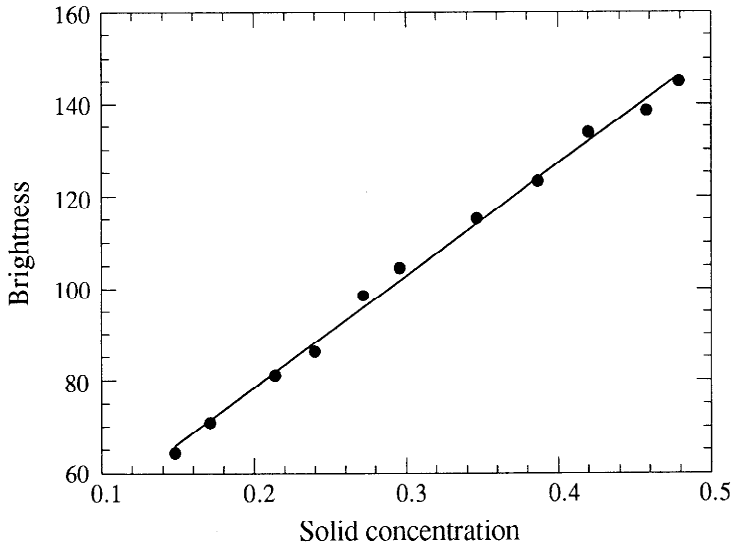

Figure 3. Averaged brightness values as a function of the mean solid concentration ϕ evaluated from the bed expansion: ●, experimental data; ——, linear regression, $B = 29.8 + 243*\phi$.

EXPERIMENTAL RESULTS

Uniform expansion

The expansion curve of the bed is given in figure 4. According to the Richardson & Zaki (1954) correlation:

$$\frac{U}{U_0} = \epsilon^n \qquad [1]$$

where U_0 is the terminal velocity of one sphere when the solid fraction is zero and $\epsilon = 1 - \phi$ is the fluid fraction. We obtained values of $n = 2.2$ and $U_0 = 0.095$ from a regression on our experimental data. This compares with the experimental terminal velocity $U_0 = 0.138$ m s^{-1} and values of the exponent from the semi-empirical Richardson & Zaki (1954) correlations $n = 2.4$. The voidage at the minimum fluidization velocity is approximately 0.5. This value is higher than the expected value

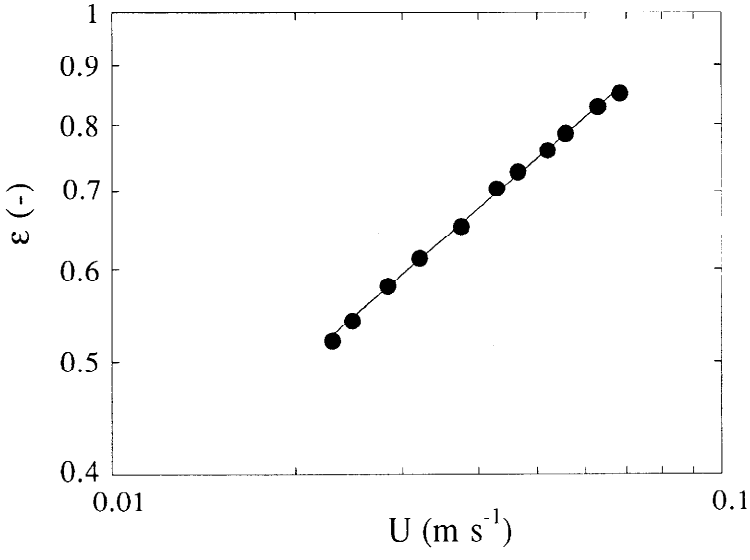

Figure 4. Expansion curve of the bed of spherical particles, $d_p = 6.35$ mm $\rho_p = 1210$ kg m^{-3}, fluidized with water.

Table 1. Experimental operating conditions

Reference number	U (cm s^{-1})	H (cm s^{-1})	ϵ	σ_ϵ
1	2.84	31	0.59	0.046
2	3.75	38	0.66	0.053
3	4.65	48	0.73	0.060
4	5.56	61	0.79	0.063
5	6.47	77	0.83	0.060

Reference numbers are kept throughout the paper.

of 0.38 which is generally found in beds of spherical particles, but in this case the effect of the big particle diameter–bed depth ratio should be relevant and can explain this discrepancy. The minimum fluidization velocity at this voidage is evaluated from the expansion curve as 0.02 m s^{-1}. Five different operating conditions were used. They are summarized in table 1.

Voidage profiles

Voidage profiles in brightness units with data at 0.1 s intervals were measured and stored. Several pixel–particle diameter ratios were tried. Significant voidage fluctuations appear to have wave lengths of several particle diameters. This motivated us to choose a pixel–particle diameter ratio small enough to have the maximum number of voidage fluctuations compatible with the definition of an image. The final value adopted was 2.7 pixel–diameter ratio corresponding to a 427 pixel–m ratio. Some examples of voidage profiles are given in figure 5 at 0.5 s intervals. It is apparent from sequences 5.1-5 that waves of bed voidage propagate from left to right; i.e. from the bottom towards the top of the bed. Although these waves have a certain stability they tend to aggregate and evolve with time. In this respect, a statistical analysis of data can provide some useful indications about the periodicity of these phenomena.

Table 1 shows the standard deviation of the voidage from the average voidage which was evaluated from the data on brightness fluctuations. To obtain values of standard deviation in voidage units we used a conversion factor $\gamma = 283$ brightness units per voidage unit which we obtained by a linear regression of average brightness values similar to that shown in figure 3. The different values of the conversion parameter are due to the different video recording conditions. It appears that fluctuations tend to increase with fluidization velocities for smaller bed expansions. In highly expanded beds the standard deviation of voidage is independent of the fluid superficial velocity.

Effect of the height from the distributor

Anderson & Jackson (1969) and Didwania & Homsy (1986) showed that voidage fluctuations originate near the distributor and increase with height above the distributor. A careful inspection of figure 5 shows that the effect of fluctuation growth with distance from the distributor is still visible in the voidage profiles, even though the voidage profiles only start at a height of 5.4 cm above the distributor. To determine the growth of the voidage fluctuations we evaluated the time average of the standard deviation of the local voidage at different bed heights over the distributor. Figure 6 provides these values of the standard deviation as a function of bed height for the lowest, the highest and the intermediate bed expansion. It appears that in all conditions, the standard deviation of the bed voidage increases steeply in the lowest section of the bed. The graph suggests an asymptotic stationary state with a constant local fluctuation level is attained in the parts of the bed away from the distributor.

Power spectra of time fluctuations of local voidage have also been evaluated at different bed heights. Figure 7 shows some of the results for the two extreme operating conditions tested. The temporal power spectra indicate that from a certain height above the distributor the differences in the frequency distribution of fluctuation can be considered negligible, supporting the above hypothesis of an asymptotic stationary state. Because the changes of the standard deviation and temporal power spectra beyond a certain height above the distributor were slight, we assumed that the voidage fluctuations were uniform in space, starting from 17 cm over the distributor for the operating condition 1 and from 20 cm over the distributor for all other operating conditions. In the rest of this paper only the data taken from these regions will be considered.

Auto-correlation analysis

Data were collected in two-dimensional arrays; one dimension was spatial and the other temporal. One-dimensional auto-correlations were carried out making the hypothesis of ergodicity and averaging in the passive dimension. The equations used are:

$$\chi_l = \frac{1}{\gamma^2 MN} \sum_{i=0}^{M-1} \sum_{k=0}^{N-l-1} \beta_{i,k}\beta_{i,k+l} \quad l = 0, 1 \ldots N-1 \qquad [2]$$

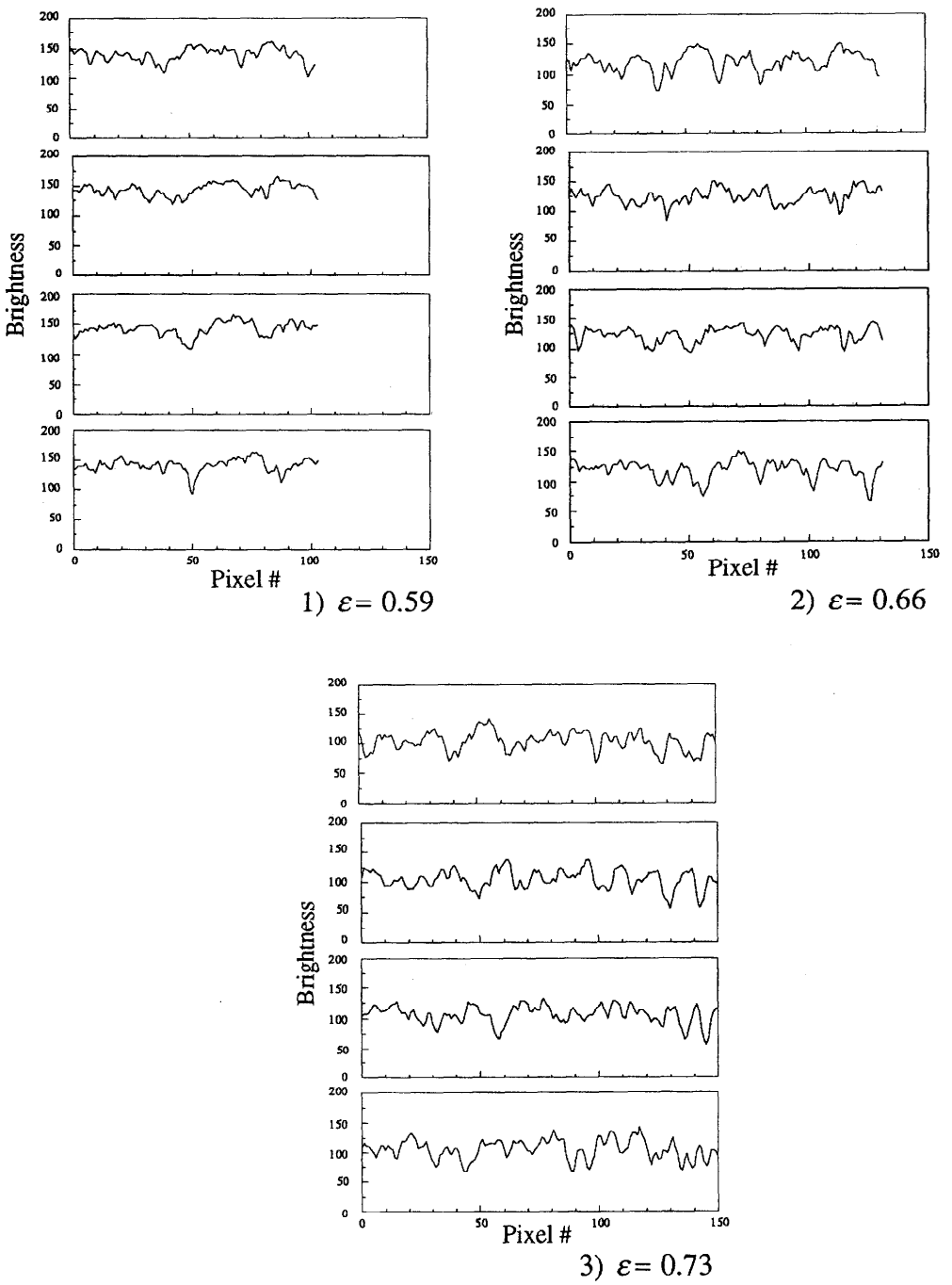

Fig. 5(a) *Caption opposite.*

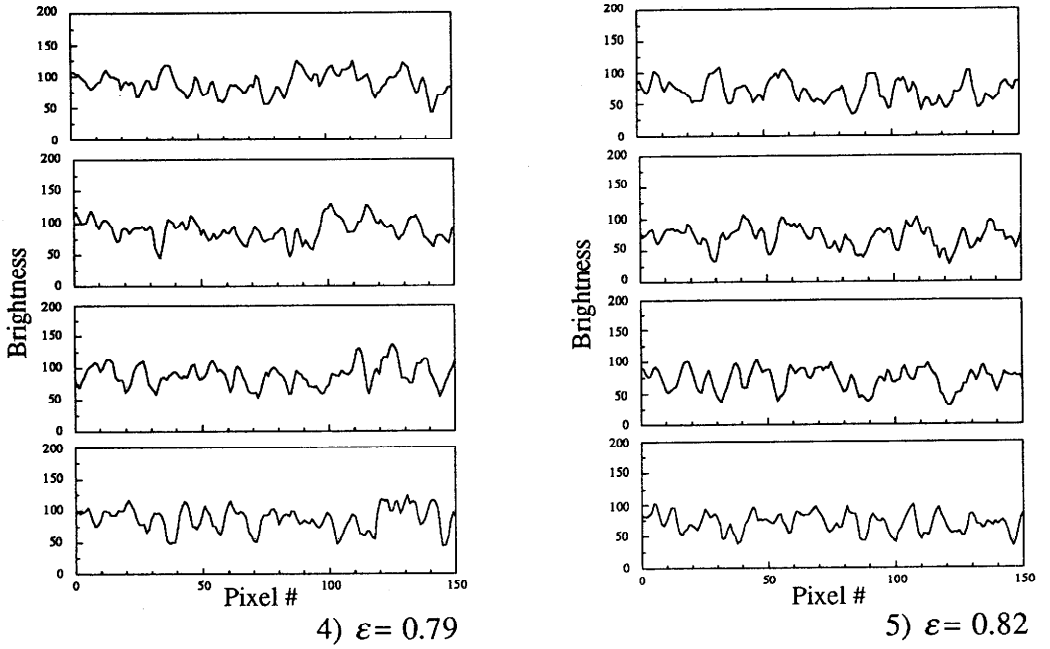

Fig. 5(b)

Figure 5. Voidage profiles in brightness units of 0.5 s intervals for the different operating conditions specified in table 1.

for spatial and

$$\tau_m = \frac{1}{\gamma^2 MN} \sum_{i=0}^{M-m-1} \sum_{k=0}^{N-1} \beta_{i,k}\beta_{i+m,k} \quad m = 0, 1 \ldots M-1 \qquad [3]$$

for temporal auto-correlations. χ_l is the lth element of the spatial auto-correlation array and τ_m is the mth element of the temporal auto-correlation array, $\beta_{i,k}$ is the difference between the mean brightness at the kth line and the mean value all over the bed at the ith time sample, γ is the brightness–voidage ratio used to convert the auto-correlation of brightness fluctuations into the

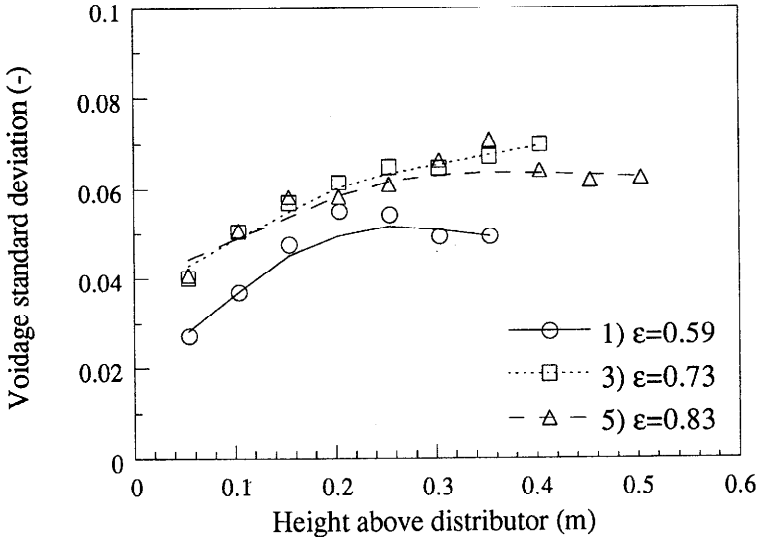

Figure 6. Local voidage standard deviation as a function of height above the distributor (see table 1 for corresponding operating conditions).

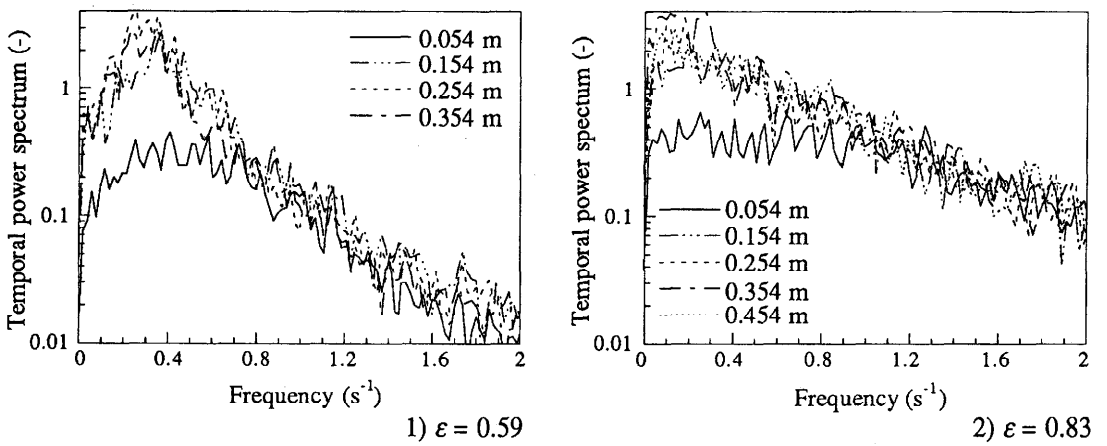

Figure 7. Temporal power spectra at different heights above the distributor (see table 1 for corresponding operating conditions).

auto-correlation of voidage fluctuations. The maximum value of N, the total line number, is limited by the maximum number (238) of lines contained in the width of the image and by the maximum height of the bed when the bed expansion is small. On the other hand the number of time samples M is limited only by the physical space in the computer memory. To improve the statistical relevance of the auto-correlation, values of χ_l and τ_m in each operating condition were calculated for 11 samples, each one lasting 30 s and then averaged.

Figures 8 and 9 provide spatial and temporal auto-correlations for three different operating conditions. The value of the auto-correlation at the origin, χ_0 or τ_0, is the square of the standard deviation. The values of the standard deviation in these cases are slightly different from those used to evaluate the standard deviation reported in table 1 which were averaged over all the bed but the dependence on the voidage appears to be the same. In all regimes, the spatial and temporal auto-correlations decay rapidly to zero. This is particularly evident at high bed expansions (plot 5 figures 8 and 9), where the signals evolve faster reducing the correlations at short distances and time as well as long ones. A decaying oscillation of the signal is evident in the temporal auto-correlations. The oscillation amplitude decreases with the bed voidage. Unfortunately, spatial correlations are not as firmly based as temporal correlations especially at small bed expansions

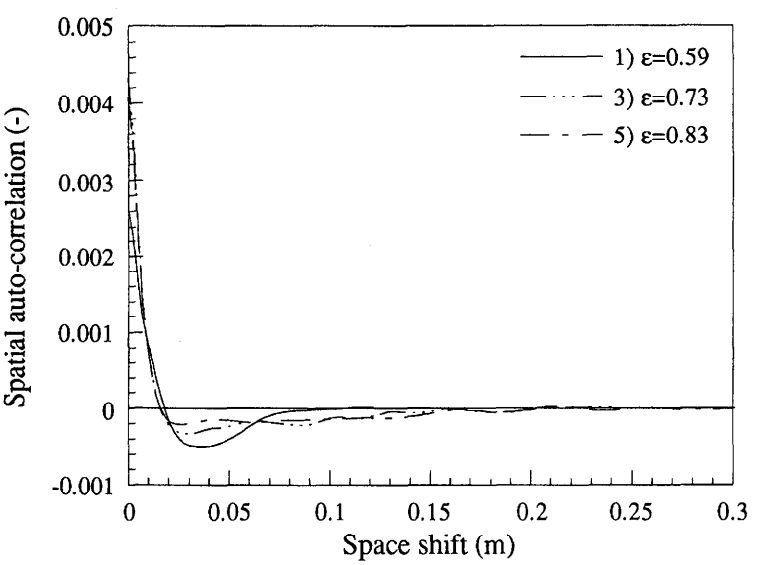

Figure 8. Spatial auto-correlation diagrams of voidage fluctuations (see table 1 for corresponding operating conditions).

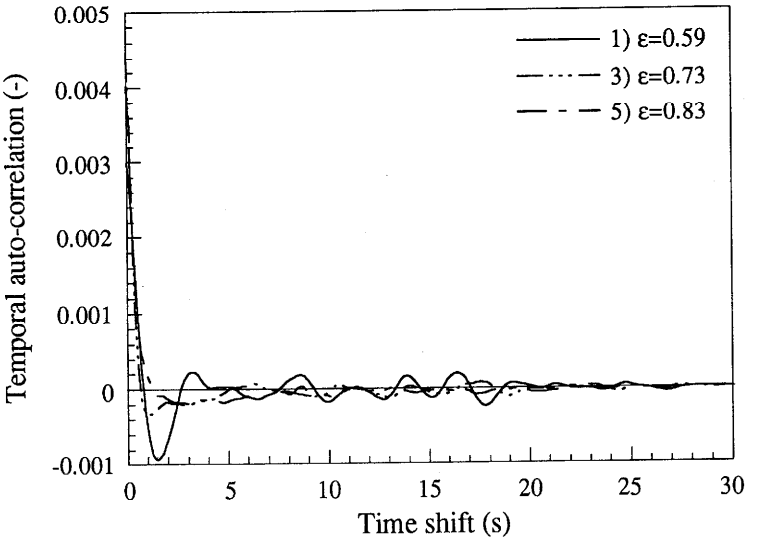

Figure 9. Temporal auto-correlation diagrams of voidage fluctuations (see table 1 for corresponding operating conditions).

(plot 1 figure 8) where the low bed height reduced considerably the length of the intervals on which voidage fluctuations could be considered stationary. In these cases the length of the sample is comparable to the length of the voidage perturbation.

Power spectra

In order to better understand the nature of the concentration waves developing within the bed, power spectra were estimated. The equations used for the periodogram estimation are:

$$X_l = \frac{1}{MN^2} \sum_{i=0}^{M-1} \sum_{k=0}^{N-1} \left| \beta_{i,k} \exp\left(-j \frac{2\pi k l}{N} \right) \right|^2 \quad [4]$$

for space and

$$T_m = \frac{1}{M^2 N} \sum_{i=0}^{M-1} \sum_{k=0}^{N-1} \left| \beta_{i,k} \exp\left(-j \frac{2\pi i m}{M} \right) \right|^2 \quad [5]$$

for time. X_l is the lth element of the spatial power spectrum array, T_m is the mth element of the temporal power spectrum array and j is the imaginary base. When needed, the arrays of data were zero padded in order to have the smallest set of elements, whose number can be expressed as a power of 2, bigger than the original one to be used by fast Fourier transform routines. Filtering and windowing of data have also been used to eliminate the irrelevant highest frequencies and to avoid numerical leakage. Values of X_l and T_m where averaged over the same 11 samples of 30 s each used to estimate the auto-correlation functions.

Power spectra for some of the operating conditions tested are given in figures 10 and 11. Spatial power spectra show predominating wavelengths between 5 and 20 cm at low voidages (plot 1 figure 10). Peaks tend to flatten at intermediate and higher voidages, indicating the presence of waves of different wavelengths (plot 3 and 5 figure 10). This is in agreement with the more chaotic behavior of the auto-correlation functions in these operating conditions. Temporal power spectra show a predominant frequency at 0.4 Hz at lower bed expansions, a range between 0.1 and 0.7 Hz at intermediate expansion and between 0.1 and 0.5 Hz at higher bed expansions. It must be noticed that values of frequencies and wavelengths obtained for high values of voidage seem unrealistic. We think that in these conditions the spectra are dominated by the effect of sampling a limited interval of space and there is not a prevailing wavelength in the waves propagating within the bed. Figure 10 shows that long waves have the greatest power, this justifies our choice of a high pixel–m ratio given previously in the sub-section on "Voidage profiles".

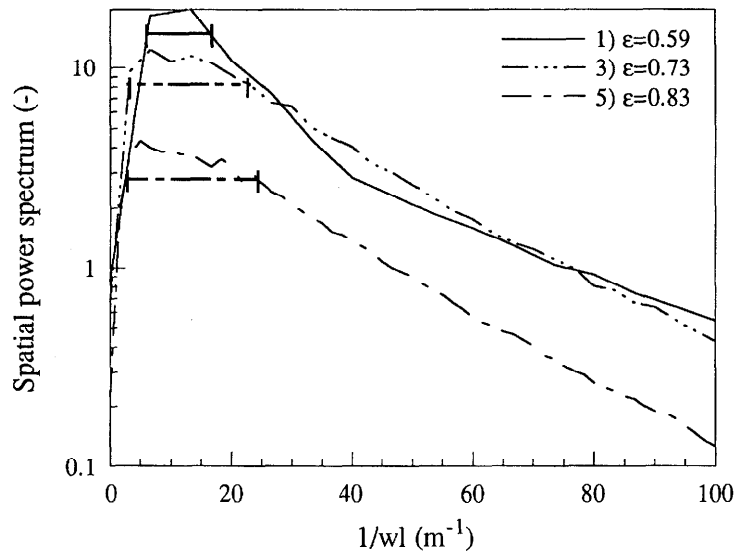

Figure 10. Spatial power spectra (see table 1 for corresponding operating conditions). Horizontal segments indicate more powerful wavelengths.

Joint spatial–temporal power spectra

Joint spatial-temporal power spectra for the five experimental conditions have been calculated using the formula:

$$\Psi_{m,l} = \sum_{i=0}^{M-1} \sum_{k=0}^{N-1} \left| \beta_{i,k} \exp\left(-j\frac{2\pi im}{M}\right) \exp\left(-j\frac{2\pi kl}{N}\right) \right|^2 \qquad [6]$$

where $\Psi_{m,l}$ is the element of the mth row and lth column in the joint spatial–temporal power spectrum array. In these cases, data arrays were zero padded in the spatial dimension and cut in the time dimension in order to obtain 256×256 source arrays to be treated by fast Fourier transform routines. In figure 12, two joint spatial–temporal power spectra are reported as an example. Analysis shows that it is not possible to match a certain wave frequency with a definite wavelength in any condition. It is rather true that at each frequency it is possible to associate a

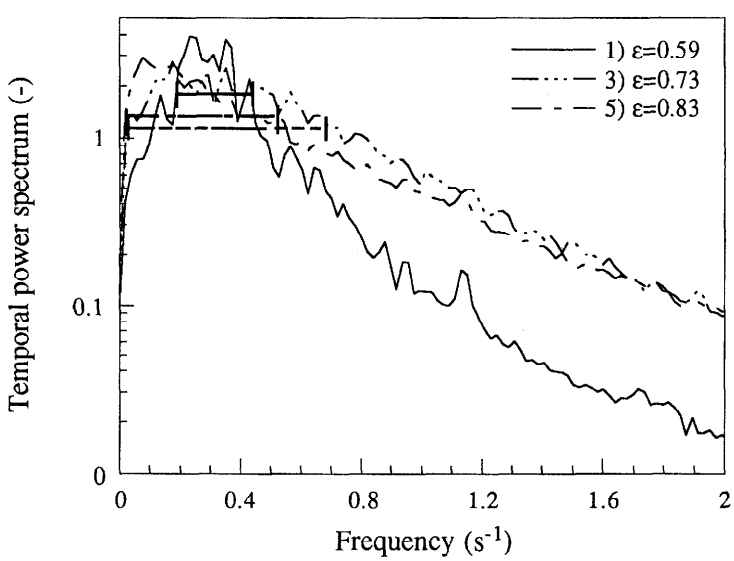

Figure 11. Temporal power spectra (see table 1 for corresponding operating conditions). Horizontal segments indicate more powerful frequencies.

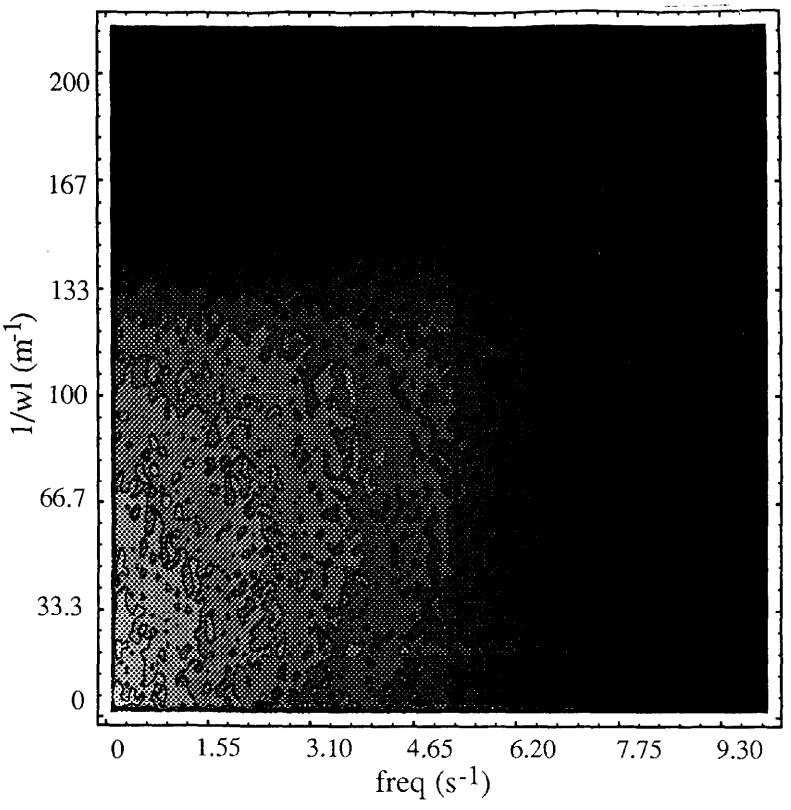

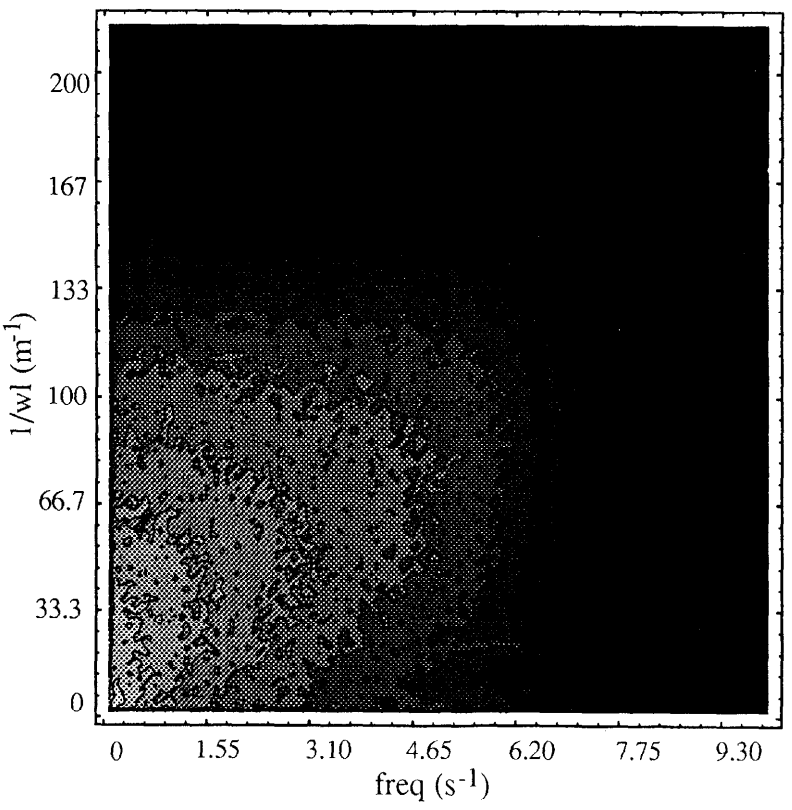

Figure 12. Joint spatial–temporal power spectra (see table 1 for corresponding operating conditions).

more or less wide range of wavelengths of considerable energy. Further confirmation of the complexity of the phenomena observed came from the evaluation of cross-correlation diagrams in time and space. Velocities were calculated from the shift in the main peak of the time and spatial cross-correlation diagram. In the two cases velocities appeared to be a function of the time interval or distance (i.e. the sampling gap) between the points of the time or spatial cross-correlation, respectively. This happens when the propagation velocity depends on the wavelength or when a considerable contribution to the cross-correlation is given by those waves whose periods or wavelengths are smaller than the sampling gap. We concluded, therefore, that this technique was not adequate to calculate wave velocities.

DISCUSSION OF EXPERIMENTAL RESULTS

Comparison with previous experimental results

As mentioned previously statistical analysis was used by other authors (Anderson & Jackson 1969; El-Kaissy & Homsy 1976; Didwania & Homsy 1981; Singh & Joseph 1991, 1995) to study the formation and the propagation of voidage disturbances within liquid-fluidized beds.

Anderson & Jackson (1969) used glass beads of a diameter smaller than those used in the present work. These authors found a variation of the amplitude of fluctuations with the distance from the distributor which is in qualitative agreement with results presented in this work. The same considerations are consistent with the tendency of the power spectra to develop a dominant frequency at larger heights above the distributor. In systems studied by Anderson & Jackson (1969), however, larger heights were required to attain a stationary value of the voidage fluctuations. Dominant frequencies were somewhat higher than those obtained in this work. The same kind of discrepancies can be found between our results and those obtained by El-Kaissy & Homsy (1976), who also used small diameter glass beads of different sizes. The dependency of voidage fluctuation on the bed expansion was also analyzed by the same authors. At high voidages, rather than the flat broadening at the dominant frequencies in the power spectra found in the present work, El-Kaissy & Homsy (1979) observed a sharp transition from low to high frequency fluctuations which corresponded to double peaked power spectra. They used cross-correlations to calculate the wave velocity. They did not notice any dependence of results upon the distance between the sampling points as observed in the present work. Didwania & Homsy (1986) report changes in the power spectra with the bed expansion which are very similar to those observed in the present work. In our experiment, however, we did not observe a sharp transition between turbulent and bubbly fluidization observed by those authors.

Singh & Joseph (1991, 1995) used a similar statistical technique on a fluidized bed with walls so closely spaced that particles could move in only two dimensions. The particle diameter was the same as that used in the present work. Voidages were around the highest values explored in this work, but smaller sampling volumes were used so that the effects of the finite size of the particles on the voidage distribution could be more accurately evaluated. Power spectra were broad banded, without a dominant frequency. The spatial auto-correlation and power spectra showed the effect of the finite size of particles, giving rise to wavelengths of the fluctuation of the area fraction on the order of the particle diameter and smaller. In particular the zero of the power of the area fraction measured in the experiments were exactly the ones predicted from the relation between the area fraction and the number density. The experimental conditions, however, were not such as to highlight the effect of longer wavelength voidage fluctuations which are observed in three-dimensional fluidized beds at voidages closer to the minimum for fluidization. We have already noted that the point spatial–temporal power spectra measured in our experiments show a wide range of wavelength for each frequency. This feature was also found in the experiments by Singh & Joseph (1991, 1995).

Comparison with theories

Wide peaks in power spectra (plots 3 and 5 in figures 8 and 9) show clearly that both wavelengths and frequencies are not narrowly defined. It is possible to identify the range of the most relevant wave numbers and frequencies in each condition. A possible choice is indicated in figures 8 and 9 by the horizontal segments. Following a conservative approach, we match the smallest values

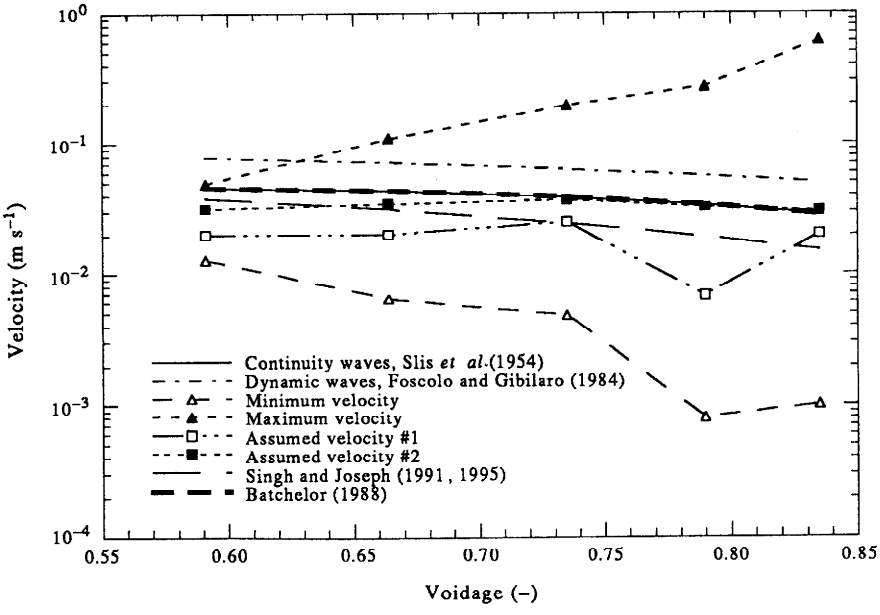

Figure 13. Comparison between experimental and theoretical values of wave velocities.

of frequency with the highest values of wave number to obtain the maximum wave velocity; the minimum wave velocity may be obtained in a similar way. The aforementioned maximum and minimum values can be seen in figure 13. In this figure we may identify a range in which the actual wave velocities are likely to be found. It is possible to carry out a less conservative procedure which gives rise to values closer to the actual velocities of the waves in the bed. In this second procedure we match the highest values of the wave number with the highest values of the frequency. Similarly, the lowest values of the wave number were matched with the lowest values of frequency. The velocities obtained in this way are also plotted in figure 13 and are referred to as "assumed" velocities 1 and 2. The two lines obtained are quite near to each other.

The considerable widening of the range of velocities obtained by the method leading to the maximum and minimum velocities for intermediate and large voidages is worth noting. This widening of dominant waves at a certain bed voidage is consistent with the hypothesis that for these conditions short and long waves coexist. It is important to keep this in mind because a change of the velocities of the dominant waves with voidage may be due not only to a change in the properties of the medium but also to the change in the characteristics of the wave.

In figure 13 experimental results are compared with some theoretical evaluations of wave velocities:

(a) Continuity wave velocities, u_ϵ, have been evaluated by combining the equation given by Slis *et al.* (1954) with [1]:

$$u_\epsilon = (1-\epsilon)\frac{dU}{d\epsilon} = n(1-\epsilon)\epsilon^{n-1}U_0 \qquad [7]$$

Measured values of n and U_0 have been used.

(b) Dynamic wave velocities, u_c, have been calculated using the following expression developed by Foscolo & Gibilaro (1984):

$$u_c = [3.2\boldsymbol{g}d_p(1-\epsilon)(\rho_s-\rho_f)/\rho_s]^{1/2} \qquad [8]$$

where $\boldsymbol{g}$ is the acceleration of gravity, d_p is the particle diameter and ρ_s and ρ_f are the particle and fluid density, respectively.

(c) Wave velocities, $u_{S\&J}$, have been evaluated according to an expression derived by Singh & Joseph (1991, 1995)

$$u_{S\&J} = \frac{4.8\tilde{g}\pi}{nU_0\lambda\epsilon^{n-1}}\left(-\frac{1}{2}+\frac{1}{2}\left\{1+\left[\frac{8(1-\epsilon)\epsilon^{2(n-1)}n^2U_0^2}{4.8d_p\tilde{g}}\Theta\left(\frac{\pi d_p}{\lambda}\right)\right]^2\right\}^{1/2}\right)^{1/2} \quad [9]$$

where $\tilde{g} = g(1-\rho_f/\rho_s)$ is the gravity acceleration corrected for the Archimedean buoyancy, λ is the wavelength and Θ is the blockage function given in the same paper. To calculate $u_{S\&J}$ from [9] at each operating condition, we used a value for the wavelength λ. This value is computed from the mean of the maximum and minimum values of the wavelength at each operating condition. For the lower, highest and intermediate voidages the maximum and minimum values can be identified by the reader from the abcissae of the extremes of the horizontal segments shown in figure 10.

(d) Wave velocities according to the Batchelor (1988) theory have also been evaluated (see [4.7] of the original paper). According to his theory, the wave velocity depends on the wavelength, the dimensionless value of the diffusion coefficient and on the system properties (density and diameter of the particles, viscosity and density of the fluid, fluidization velocity and voidage). We obtained the wavelengths from measurements by the procedure described in the foregoing paragraph. The diffusion coefficient was evaluated using a stability criterion [4.10] given in the original paper; this criterion depends on the same variables used to evaluate the wave velocities. Therefore, the same value of the wavelength gives rise to a value of the dimensionless diffusion coefficient corresponding to transition from uniform homogeneous to heterogeneous flow occurs. In fact, the value of the diffusion coefficient is not known and some method must be employed if the theory is to be compared with experiments.

Almost all the values of wave velocities obtained according to the different theories fall within the wider range of possible experimental wave velocities (figure 13). In general, theoretical values are close to the "assumed" velocities 1 and 2. Theoretical values, however, show a slight but steady decrease of the velocity with voidage. The two "assumed" velocities show constant, if not slightly increasing, values. The degree of uncertainty in the experimental data and in their interpretation does not allow us to reject or discriminate between theories. The curve of wave velocity versus voidage obtained from Batchelor's (1988) theory is coincident with the curve for continuity waves (figure 13). This result is not surprising. It could have been obtained also by applying the relationship which correlates the wavelength, λ, with the wave velocity, w, obtained by Wallis (1969) from a linearized stability analysis of fluidized beds:

$$\left(\frac{2\pi}{\lambda}\right)^2 = \left[\frac{4.8g(\rho_s-\rho_f)}{2wnU_0\rho_s\epsilon^{n-1}}\right]^2\left(\frac{u_c^2-w^2}{w^2-u_c^2}\right) \quad [10]$$

Wallis' (1969) theory predicts values for wave velocity which differ consistently from the continuity wave velocity only in the case of very short wavelengths. This was already noted by Foscolo & Gibilaro (1987) in their interpretation of experimental data by El-Kaissy & Homsy (1976). The high frequencies for which the two theories begin to differ can be estimated from [10] under the assumption that the coefficient in round brackets is of order one:

$$\nu = \frac{w}{\lambda} = O\left(\frac{1.2}{\pi}\frac{g(\rho_s-\rho_f)}{nU_0\rho_s\epsilon^{n-1}}\right). \quad [11]$$

Using measured values from our fluidized bed we find that the value of the frequency for which $w \neq u_c$ significantly are on the order of $10\,s^{-1}$, which is considerably bigger than we have found in our experiments.

It is apparent from figure 13 that the dynamic wave velocity predicted by Foscolo & Gibilaro (1984) is always bigger than the continuity wave velocity. According to the Wallis criterion, which Foscolo & Gibilaro (1984) use, homogeneous fluidization should be stable when the continuity wave velocity u_c is less than the dynamic wave velocity u_c:

$$u_c < u_c. \quad [12]$$

Equations [10] and [12] show that the condition for the waves to exist is equivalent to the requirement that λ is real

$$u_e \leqslant w \leqslant u_t. \qquad [13]$$

In the one-dimensional theory of linear waves (Wallis 1969; Gibilaro *et al.* 1988) a travelling wave of voidage is expressed by:

$$\epsilon = A \exp\left(\alpha t + 2\pi i \frac{z - wt}{\lambda}\right) \qquad [14]$$

where z is the spatial co-ordinate, A is the wave amplitude and α is the growth rate. Following Wallis (1969), one finds that:

$$\alpha = \frac{2.4g(\rho_s - \rho_f)}{wnU_0\rho_s\epsilon^{n-1}}(u_t - w). \qquad [15]$$

For "comparative purposes" Gibilaro *et al.* (1988) calculate α for waves of $\lambda = 20d_p$ (using [10] to evaluate w) and call this value α^*. They state that fluidized beds for which

$$-0.7 < \alpha^* < 0.7 \qquad [16]$$

are indeterminately stable. As they explain, this corresponds to waves which decrease their amplitude less than one half or increase it less than twice in one second and, therefore, they suppose that only outside the range given by [16] the behavior of the bed will be unambiguously particulate or aggregate. The range of α^* given by [15] in our experiments is $-0.4 < \alpha^* < -0.2$ which is well within the range of indeterminate stability [16]. Negative values of α lead to stability and are consistent with the predicted stability of uniform fluidization given by [12] but, according to Gibilaro *et al.* (1988), their modulus is too small to induce a determinate particulate expansion.

It is of interest that independent values of wave velocities obtained from Singh & Joseph (1991, 1995) and from Batchelor (1988) are both consistent with the Wallis criterion [12]. In no case can linear theories explain the formation of saturated waves. The non-linear approach of Fanucci *et al.* (1979) to the stability of uniform fluidization and to the propagation of voidage disturbances might provide some suggestion. One result of their analysis on a non-linear hyperbolic model is that the condition [12], which is necessary for dumped waves in a linear theory, need not imply stability and could allow growing waves which break into shocks. This would invalidate [13] and justify experimental wave velocities bigger than u_t as shown in figure 13. On the other hand, studies of a non-hyperbolic model of a fluidized suspension (Liu 1983; Needham & Merkin 1983) are consistent with [12] and give some non-linear stabilization of the growth of voidage perturbations. This might explain the existence of the saturated waves of finite amplitude observed in this and in previous works (Anderson & Jackson 1969; El-Kaissy & Homsy 1976; Didwania & Homsy 1981; Ham *et al.* 1990). In this case, results of different theoretical analyses are in contradiction and do not help in the full comprehension of all the phenomena observed.

CONCLUSIONS

Fluctuations of voidage have been detected in a two-dimensional fluidized bed and correlated to the variations in the average brightness values measured with a digital video camera. We did a statistical analysis of the collected data at operating conditions near to the minimum for fluidization.

The calculation of temporal power spectra and standard deviation at different heights above the distributor showed that voidage fluctuations develop and grow with height near to the distributor. At distances larger than 20 cm from the distributor, however, voidage fluctuations reach a stationary state. In this region, with our experimental technique, we were able to obtain spatial correlations, spatial power spectra and joint spatial–temporal power spectra as well as time correlation and temporal power spectra.

The analysis of auto-correlations and power spectra indicates that the characteristics of the signal become increasingly chaotic as the fluidization velocity increases and higher voidages are

interrogated. Joint spatial–temporal power spectra show that there are no monochromatic waves; for each frequency a band of wavelengths can be found.

Our results are in qualitative agreement with those by Anderson & Jackson (1967), El-Kaissy & Homsy (1976) and Didwania & Homsy (1981), except that bubbling behaviors observed by them are not observed in our experiments. In spite of the different conditions tested and the different wavelengths studied, our results agree with Singh & Joseph (1991, 1995) with regard to the shape of the joint spatial–temporal power spectrum.

From the evaluation of dominant frequencies and wavelengths we calculated a wide range of possible wave velocities corresponding to different operating conditions. We also evaluated the most likely value of the wave velocity and compared our results with those obtained from the work of Slis *et al.* (1954), Foscolo & Gibilaro (1984), Batchelor (1988) and Singh & Joseph (1991, 1995). The degree of uncertainty in the experimental data and their interpretation does not allow one to discriminate between theories. We notice, however, that values of velocities obtained by Singh & Joseph (1991, 1995) and those obtained by Batchelor are consistent with the Wallis (1969) criterion.

Acknowledgements—We wish to thank Dr P. Singh for useful discussion, in particular on the statistical treatment of data, both in the early stages of this work and in the final writing of the paper. The sojourn of one of us (M.P.) at the Aerospace Engineering and Mechanics Department of the University of Minnesota was made possible by a travel grant from the University of Naples "Federico II". This work was supported by the NSF, Fluid, Particulate and Hydraulic Systems, by the U.S. Army, Mathematics and AHPCRC, by the DOE, Department of Basic Energy Sciences, the Minnesota Supercomputer Institute and the Schlumberger Foundation.

REFERENCES

ANDERSON, T. B. & JACKSON, R. 1969 A fluid mechanical description of fluidized beds. *IEC Fundament.* **8,** 137 144.

BATCHELOR, G. K. 1988 A new theory of the instability of a uniform fluidized bed. *J. Fluid Mech.*, **193,** 75–110.

DIDWANIA, A. K. & HOMSY, G. M. 1981 Flow regimes and flow transitions in liquid fluidized bed. *Int. J. Multiphase Flow* **7,** 563–580.

EL-KAISSY, M. M. & HOMSY, G. M. 1976 Instability waves and the origin of bubbles in fluidized beds. *Int. J. Multiphase Flow* **2,** 379–395.

FANUCCI J. B., NESS N. and YEN R.-H. 1981 Structure of shock waves in gas–particulate fluidized beds. *Phys. Fluids* **24,** 1944–1954.

FORTES, A. F., JOSEPH, D. D. & LUNDGREN, T. S. 1987 Nonlinear mechanics of fluidization of beds of spherical particles. *J. Fluid Mech.* **177,** 467–483.

FOSCOLO, P. U. & GIBILARO, L. G. 1984 A fully predictive criterion for the transition between particulate and aggregate fluidization. *Chem. Engng Sci.* **39,** 1667–1675.

FOSCOLO, P. U. & GIBILARO, L. G. 1987 Fluid dynamic stability of fluidised suspensions: the particle bed model. *Chem. Engng Sci.* **42,** 1489–1500.

GIBILARO, L. G., DIFELICE, R., FOSCOLO, P. U. & WALDRAM, S. P. 1988 Fluidization quality: a criterion for determinate stability. *Chem. Engng J.* **37,** 25–33.

HAM, J. M., THOMAS, S., GUAZZELLI, E., HOMSY, G. M. & ANSELMET, M. C. 1990. An experimental study of the stability of liquid-fluidized beds. *Int. J. Multiphase Flow* **16,** 171–185.

JOSEPH, D. D., SINGH, P. & FORTES, A. 1992 Nonlinear and finite size effects in fluidized suspensions. In *Particulate Two-phase Flow* (Edited by ROCCO M. C.), Chap. 10. Butterworth–Heinemann, Oxford.

LIU, J. T. C. 1983 Nonlinear unstable wave disturbances in fluidized beds. *Proc. R. Soc. Lond.*, *A* **389,** 331–347.

NEEDHAM, D. J. & MERKIN, J. H. 1983 The propagation of a voidage disturbance in a uniformly fluidized bed. *J. Fluid Mech.* **131,** 427–454.

RICHARDSON, J. F. & ZAKI, W. N. 1954 Sedimentation and fluidisation: Part I. *Trans. Inst. Chem. Engrs* **32,** 35–53.

SINGH, P. & JOSEPH, D. D. 1991 *Finite Size Effects in Fluidized Beds in Liquid–Solid Flow. FED 118* (Edited by ROCCO, M. C. & MEGASUME, T.). pp. 77–86. American Society of Mechanical Engineers.

SINGH, P. & JOSEPH, D. D. 1995 Dynamics of fluidized suspensions of spheres of finite size. *J. Fluid Mech.* In press.

SLIS, P. L., WILLEMSE, T. W. & KRAMERS, H. 1959 The response of the level of a liquid fluidised bed to a sudden change in the fluidizing velocity. *Appl. Sci. Res.* **A8,** 209–218.

VOLPICELLI, G., MASSIMILLA, L. & ZENZ, F. A. 1966 Nonhomogeneities in solid–liquid fluidization. *Chem. Engng Prog. Symp. Ser.* **62,** 42–50.

WALLIS, G. B. 1969 *One-dimensional Two-phase Flow.* McGraw–Hill, New York.